Step free energies, surface stress, and adsorbate interactions for Cl-Si(100) at 700 K

G. J. Xu, S. V. Khare, Koji S. Nakayama, C. M. Aldao,* and J. H. Weaver
Department of Materials Science and Engineering and Frederick Seitz Materials Research Laboratory, University of Illinois at Urbana-Champaign, Urbana, Illinois 61801, USA
(Received 14 August 2003; published 12 December 2003)

The evolution and equilibrium morphology of Si(100) with 0.1 monolayer of adsorbed Cl was studied at 700 K with variable temperature scanning tunneling microscopy. Chlorine caused surface roughening with monolayer pits and regrowth islands. The aspect ratio of these features then increased with their size because of the surface-stress anisotropy. By analyzing the equilibrium feature shape as a function of size, we found that the ratio of step free energies for *A*- and *B*-type steps was $F_b/F_a=2.44$ for regrowth islands and 3.33 for pits. These ratios are higher than for clean Si(100), $F_b/F_a=2.13$, because the steps are destabilized.

DOI: 10.1103/PhysRevB.68.235318 PACS number(s): 68.35.Ja, 68.35.Md, 68.37.Ef, 81.65.Cf

I. INTRODUCTION

Clean Si(100)-(2×1) and the energies of its two inequivalent steps have been studied extensively.[1] Step free energies are essential to the understanding of many surface properties, including surface equilibrium morphologies and interactions between surface particles. Swartzentruber *et al.*[2] determined the distribution of kink separations and kink lengths, Bartelt *et al.*[3] measured step fluctuations and equilibrium island shapes, and Zandvliet and co-workers[1,4] examined the statistics of step profiles. Zielasek and co-workers[5] studied the intrinsic surface-stress anisotropy and island shapes near thermal equilibrium. Adsorbates can be expected to modify the characteristics of steps, and this paper shows that it is possible to quantify changes in step free energies.

The halogen-Si(100) systems are of great importance scientifically and technologically because halogen-based etching is used throughout the microelectronics industry. Hence, the processes and consequences of the production of pits and regrowth islands on Si(100)-(2×1) have attracted extensive attention.[6–13] To date, however, there have been no studies of the step free energies on Si(100) with halogen adatoms, though such investigations would provide insights into the effects of a large class of adsorbates.

In this paper, we examine the influence of 0.1 ML of Cl on Si(100) at 700 K. At this temperature, Cl causes surface roughening that is manifested as extended regrowth islands and pits, but the temperature is too low to activate etching via dihalide desorption.[7,9,10] Variable temperature scanning tunneling microscopy (STM), was used to determine the equilibrium shapes of islands and pits as a function of their sizes. Analysis then showed that the aspect ratio of both islands and pits increased with their sizes. Within the theoretical framework proposed by Li *et al.*,[14] where the equilibrium island shape is determined by both step free energies and surface stress, we then determined the ratio of step free energies for S_A and S_B steps and the ratio between step free energy and surface strain energy. Our emphasis on roughened surfaces provides a new way to study surface energetics, complementing previous work that focused on islands established during the early stages of epitaxial growth[3,5,15–18] and involving real time investigation in true equilibrium.

II. EXPERIMENT

The experiments were carried out in an ultrahigh vacuum system with an Omicron variable temperature STM and an appended sample preparation chamber (operating pressure $<4\times10^{-11}$ Torr). The Si wafers were *p* type, *B* doped to 0.01–0.012 Ω cm, and oriented within 0.5° of (100) with miscut along [100]. Clean surfaces were prepared by degassing at 875 K for 12 h and then heating to 1475 K for 90 s at $<1\times10^{-10}$ Torr. The surface defect area was $\sim$0.01–0.02 ML, primarily in the form of dimer vacancies.

A solid electrochemical cell derived from AgCl doped with $CdCl_2$ provided a flux of Cl_2 when a voltage was applied. Clean Si surfaces were exposed at room temperature to achieve 0.1 ML coverage. The adsorbate concentration was determined directly from the STM images since Si dimers with Cl can be distinguished from bare dimers.[11,19] The samples were then heated to 700 K for extended imaging.

An optical pyrometer was used to monitor the sample temperature, and a relation between temperature and heating power was determined. During scanning, the temperature was adjusted by varying the heating power. Filled-state images were acquired with Pt/Ir tips in the constant current mode. In our analysis, we considered only pits and islands that were at least $\sim$50 nm away from nearest neighbors and steps to minimize feature-feature and feature-step interactions.

III. RESULTS AND DISCUSSION

The image in Fig. 1 represents the equilibrium surface morphology of 0.1 ML Cl-Si(100). It was acquired after the sample had been at 700 K for 4.6 h. Chlorine causes the surface to roughen at this temperature as Si atoms are ejected onto the terrace and dimer vacancies are created.[7–9] These species are mobile and their coalescence produces large regrowth islands (RI's) and pits. At 700 K, repetitive scanning of the same area shows that dynamic equilibrium was reached within a few hours at 700 K. Subsequent imaging showed that individual features continued to undergo changes, as expected, with the appearance/disappearance of

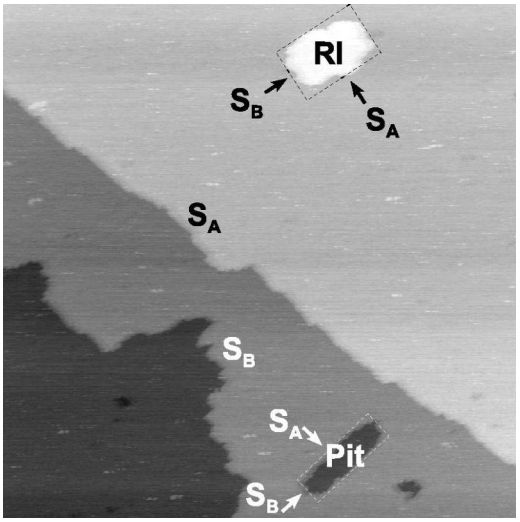

FIG. 1. Representative image of the equilibrium morphology for 0.1 ML Cl-Si(100) at 700 K (300×300 nm^2) showing three terraces that descend from upper right to lower left. S_A steps are straight and almost unchanged compared to clean Si(100), while S_B steps have large peninsulas, gulfs, and even overhangs (not shown). Regrowth islands, RI's, and pits are bounded by their own S_A and S_B steps.

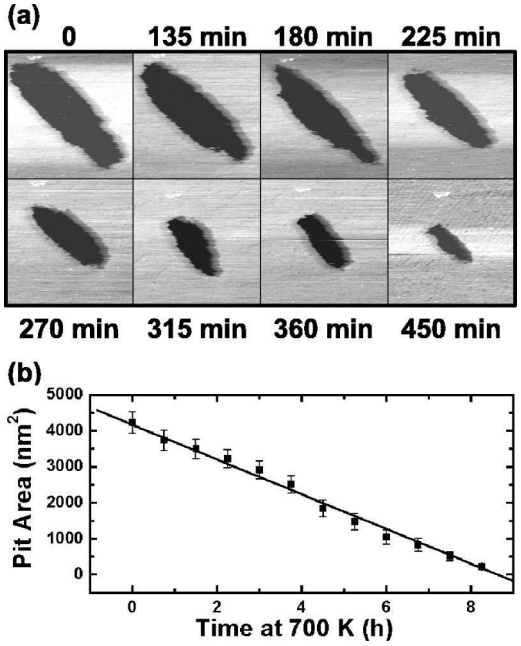

FIG. 2. Most large features fluctuate in size and shape for a surface in dynamic equilibrium at 700 K, but the images in (a) capture the decay of a large pit. The decay rate in (b) is independent of pit size and local environment, implying a detachment-limited process as dimer vacancies escape into the surrounding terrace.

small RI's and pits and the growth and decay of larger ones.[10]

The image in Fig. 1 shows two steps with the S_A step running parallel to the dimer row direction and S_B running perpendicular to it. There is one RI and one large pit, and both are bounded by S_A and S_B steps. The RI is elongated perpendicular to the substrate dimer row direction; it is ~1484 nm^2 in area and ~208 nm in perimeter. The pit extends along the substrate dimer row direction; it is ~813 nm^2 in area and ~180 nm in perimeter. Small RIs and pits are not visible at this resolution as the scan area is 300×300 nm^2. Such features are not considered in our analysis because they undergo rapid fluctuations under conditions of dynamic equilibrium. Comparison to clean Si(100) shows that the effect of 0.1 ML Cl on the step profiles is profound. For the clean surface, S_A steps have a low kink density while S_B steps are much less regular because the energy needed to form a kink in an S_B step is much lower than that for an S_A step. Here, the S_A steps have similar profiles to those on the clean surface. However, the development of large peninsulas and gulfs in S_B steps demonstrates that even small amounts of Cl change the effective substrate dimer-dimer interactions.

The shape of the RIs for Cl-Si(100) is also quite different from what has been observed in Si(100) homoepitaxy. Zielasek *et al.*[5] reported islands that were elliptical at small size and "American-football"-like at larger size. In contrast, those observed here are much smaller and are approximately rectangular with the S_A step length bounding an island being greater than the S_B step length. For example, the lengths of the S_A and S_B steps for the island in Fig. 1 are 58 nm and 34 nm (aspect ratio ~1.7). Hence, the free energy of the S_A steps, F_a, is smaller than that of S_B steps, F_b. This is also manifest in pit profiles because they elongate along S_A steps. For the large pit in Fig. 1, the step lengths are 59 nm and 19 nm, respectively (aspect ratio is ~3.1).

While most large features fluctuated in size but survived under conditions of dynamic equilibrium, others simply decayed. Figure 2(a) shows a series of images (120×120 nm^2) that focus on the decay of one such pit. Over the course of 450 min, it shrank from ~4234 nm^2 to ~120 nm^2 and it had disappeared 90 min later. Figure 2(b) shows that the area decreased linearly with time. This implies that mass transport associated with decay is limited by the detachment of the dimer vacancies from step edges.[9,20] The area decay rate $dA/dt=502\pm15$ nm^2/h is proportional to the product of average step mobility and average step stiffness at 700 K.[21]

The shape of a two-dimensional island on a surface is determined by the ratio of its step free energies, in the absence of surface-stress anisotropy.[22] For Si(100), dimerization results in a very anisotropic surface stress that is tensile along the dimer bond and compressive along the dimer row.[23] Li *et al.*[14] studied the effect of stress on the equilibrium shape of an island using continuum elasticity theory. They found that the surface stress anisotropy influences the island shape, and that the island aspect ratio depends on the island size. With this theoretical model, Zielasek *et al.*[5] studied surface-stress-induced island shape transitions in Si(100), and Middel *et al.*[24] investigated the surface-stress anisotropy in Ge(100). We can extend these analyses to consider the influence of adsorbates on the surface-stress anisotropy. We focus on the effects of 0.1 ML of Cl since feature-feature interaction is unavoidable at higher coverage where the feature density is high and the features are small.[10]

The Si(100)-(2×1) surface has twofold symmetry and

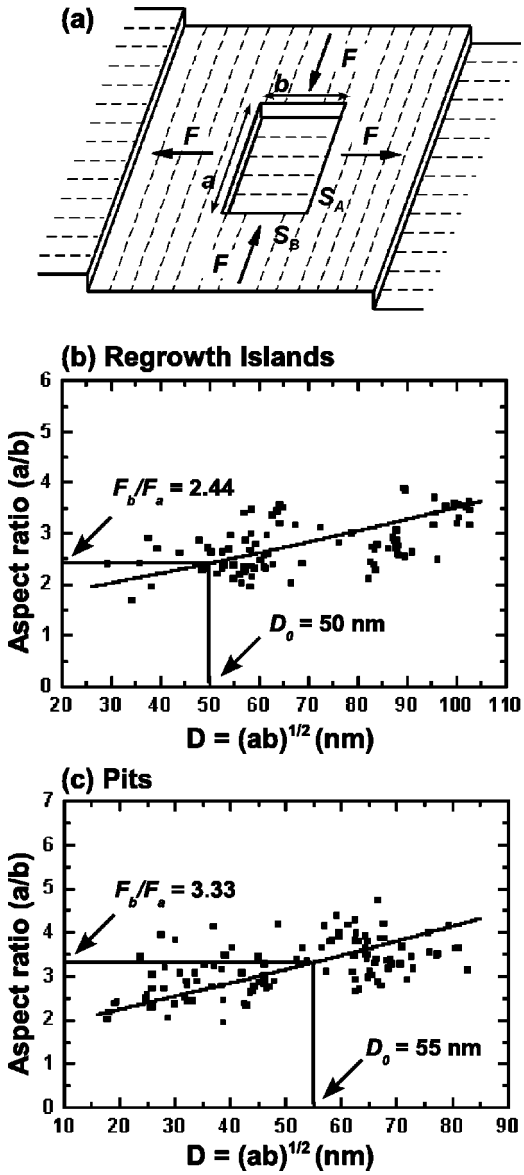

FIG. 3. (a) shows a schematic of 2D pits with a rectangular shape of length a and width b. The dashed lines signify the direction of dimer rows. F represents the elastic force monopole along the pit periphery induced by surface-stress anisotropy, and it points outward along the S_A steps and inward along the S_B steps. The aspect ratios of regrowth islands (b) and pits (c) show an increase with increased feature size. The areas range from ~ 845 nm^2 to ~ 10543 nm^2 for islands and from ~ 315 nm^2 to ~ 6836 nm^2 for pits. The slanted solid lines represent the best fit to the theoretical model, yielding $\alpha = 6.8 \pm 0.7$ and $\beta = 0.64 \pm 0.05$ for islands and $\alpha = 6.8 \pm 0.7$ and $\beta = 0.55 \pm 0.06$ for pits. $\alpha = \sqrt{F_a F_b}/E_s$ is the ratio of the average step energy to the strain energy and $\beta = \sqrt{F_a/F_b}$ is the ratio of step free energies. From the model for step free energies, optimum ratios of $F_b/F_a = 2.44$ and 3.33 indicate specific sizes of $D_0 \approx 50$ and 55 nm for regrowth islands and pits. The aspect ratio is the same as the step free energy ratio.

biaxial strain so we approximated the feature shapes as rectangles. Figure 3(a) is a schematic view of two-dimensional (2D) rectangular pits of length a and width b. F represents the elastic force monopole along the pit periphery induced by the surface-stress anisotropy. Note that the force monopole points outward along the S_A steps and inward along the S_B steps. Figures 3(b) and 3(c) show the aspect ratio, $c^2 = a/b$, of RI's and pits as a function of their size, $D = \sqrt{ab}$. The measurement was done over a large area during a time lapse from ~ 6 h to ~ 72 h after the surface reached 700 K. The results of Figs. 3(b) and 3(c) represent the analysis of 90 RI's and 107 pits that were far away from other features and step edges. The sizes range from ~ 845 nm^2 to $\sim 10\,543$ nm^2 for RI's and from ~ 315 nm^2 to ~ 6836 nm^2 for pits. While there is scatter in the experimental points in Figs. 3(b) and 3(c), the increase in aspect ratio with size is apparent. The slanted solid lines represent the best fit to the model described below.

The total free energy for an individual feature, including step and strain energies, can be calculated as

$$F_{total} = F_{step} + F_{stress} = 2aF_a + 2bF_b + \frac{1}{2}\int\int \vec{u}[\vec{r}_1, \vec{F}(\vec{r}_2)] \cdot \vec{F}(\vec{r}_1) d\vec{r}_1 d\vec{r}_2, \quad (1)$$

where $\vec{F}$ is the stress anisotropy [it is pointing outward along S_A steps and inward along S_B steps, see Fig. 3(a)], F_a and F_b are the unit length step free energies for S_A and S_B steps, and $\vec{u}[\vec{r}_1, \vec{F}(\vec{r}_2)]$ is the displacement at point $\vec{r}_1$ induced by the force $\vec{F}$ at point $\vec{r}_2$. Adapting from Li *et al.*,[14] the total free energy can be written

$$\frac{F_{total}}{E_s} = \frac{2aF_a + 2bF_b}{E_s} + \left[PG(c) - P \times 2(1-\nu) \ln \frac{D}{a_0} \right] = P \times \left[\alpha \frac{\beta^2 c^2 + 1}{\beta c^2 + \beta} + G(c) \right] - P \times 2(1-\nu) \ln \frac{D}{a_0}, \quad (2)$$

where $E_s = [(1+\nu)/2\pi\mu]F^2$, i.e., the interaction energy of two parallel force monopoles at unit separation. $F = |\vec{F}|$ is the absolute value of surface-stress anisotropy, $P = 2(a+b)$ is the perimeter of the island or pit, $\alpha = \sqrt{F_a F_b}/E_s$ is the ratio of the average step energy to the unit strain energy, $\beta = \sqrt{F_a/F_b}$ corresponds to the ratio of step free energies of S_A and S_B steps, μ and ν are the Young's modulus and Poisson ratio for silicon, and a_0 is a cutoff length in the range of the surface lattice constant. Note that the island strain energy has two terms, both proportional to the perimeter P but with different signs. $G(c)$ is a dimensionless geometric factor given by

$$G(c)=\frac{1}{2\left(c+\frac{1}{c}\right)}\left\{2(1-\nu)\left(c\ln\frac{\sqrt{c^2+\frac{1}{c^2}}+c}{\sqrt{c^2+\frac{1}{c^2}}-c}+\frac{1}{c}\ln\frac{\sqrt{c^2+\frac{1}{c^2}}+\frac{1}{c}}{\sqrt{c^2+\frac{1}{c^2}}-\frac{1}{c}}-2c\ln\frac{c}{e}-2\frac{1}{c}\ln\frac{1}{ce}\right)+4\left[(1-4\nu)\left(c+\frac{1}{c}\right)-2(1-3\nu)\sqrt{c^2+\frac{1}{c^2}}\right]\right\}. \tag{3}$$

The aspect ratio $c^2=a/b$ for the features studied falls in the range 2–4.5 and $G(c)$ lies in the range 3.7–5.7.

This model of the free energy of a pit or island predicts that there should be a favored aspect ratio for a given feature size at a given temperature since F_a, F_b, and E_s are constant. We can fit the theoretical curves to experiment by adjusting the values of α and β and using $\mu=1.5\times10^{11}$ N/m^2, $\nu=0.17$,[25] and $a_0=3.84$ Å for Cl-Si(100). The best fits in Fig. 3 correspond to $\alpha=6.8\pm0.7$ and $\beta=0.64\pm0.05$ for RI's and $\alpha=6.8\pm0.7$ and $\beta=0.55\pm0.06$ for pits. The ratio of step free energies is then $F_b/F_a=2.44$ for islands and 3.33 for pits.

It is instructive to compare these results to those for clean Si(100) where the step formation energies have been studied extensively and the values proposed by Zandvliet and co-workers[26,27] are well accepted, namely, $E_a=52$ and $E_b=120$ meV/(2a). Using these values, we can determine the step free energy since entropy $S_{a,b}$ can be included as $F_{a,b}=E_{a,b}-TS_{a,b}$. At 700 K, the entropy term contributes about 5 meV/(2a) for S_A steps and 20 meV/(2a) for S_B steps (see Ref. 27 for a detailed discussion). Therefore, $F_a=47$ and $F_b=100$ meV/(2a) for the clean surface at 700 K and $F_b/F_a=2.13$. This explains why it is easier to form kinks on S_B than on S_A steps so that S_B steps are rough while S_A steps are straight. The effect of Cl is to increase the values of F_b/F_a, thereby producing S_B steps that are rougher than those on the clean surface while leaving the S_A steps little changed.

It is intriguing that the ratios of step free energies are different for islands and pits. This difference reflects the fact that the adsorbate coverages are different on the three exposed layers of Si(100), namely on the regrowth islands, the main terrace, and in the pits. As reported by Nakayama *et al.*,[19] the coverage is the highest on the main terrace and the lowest on the islands. Hence, steps the surrounding pits are more destabilized than those surrounding the islands because of the higher Cl concentration.

To study the effect of Cl on the surface-stress anisotropy, we compare the ratio between step free energy and strain energy for clean Si(100) and Cl-Si(100). For clean Si(100)-(2×1), Zandvliet and Elswijk analyzed the terrace width distribution and determined the stress anisotropy $F=80$–130 meV/Å^2.[26] Zielasek *et al.*[5] used the above model to study the shape of an island during homoepitaxial growth. They found that $F=68\pm3$ meV/Å^2 at 1128 K, $F=84\pm4$ meV/Å^2 at 968 K, and that the stress anisotropy increased with decreasing temperature. Using the stress anisotropy value $F=80$ meV/Å^2, we derived $\alpha=7.0$ for clean Si(100)-(2×1). The present analyses yield $\alpha=\sqrt{F_aF_b}/E_s=6.8$ for the Cl modified Si(100), which is comparable to that of the clean surface. This means that Cl adsorbates have a similar effect on the step free energies and the intrinsic surface-stress.

The contribution of strain energy to the total free energy appears as two terms with opposite sign in Eq. (2), namely, $PG(c)-P\times2(1-\nu)\ln(D/a_0)$. For small islands (pits), the first term, $PG(c)$, dominates and the contribution of the strain energy to the total energy is positive. Consequently, the minimization of the total free energy requires a smaller perimeter and a more isotropic shape than what would be predicted if only the step energies were considered. Conversely, the second term dominates for large islands (pits), and the contribution of the strain energy is negative. Thus, the strain energy favors a larger perimeter and a larger aspect ratio.

It is clear from Figs. 3(b) and 3(c) that the aspect ratios of RI's and pits increase with feature size. In contrast, the ratio of step free energies is constant at a given temperature. From the best fit, the ratios of step free energies yield a specific size of $D_0\approx50$ and 55 nm for islands and pits, where the step free energy ratio is the same as the aspect ratio. Minimization of the second term in Eq. (2), $PG(c)-P\times2(1-\nu)\ln(D/a_0)$, which represents the contribution from surface-strain energy, also results in the same values.

The value of surface-stress anisotropy has not been determined for Cl-Si(100), and the absolute step free energies cannot be precisely derived. However, they are expected to be smaller than those of clean Si(100) because Cl destabilizes dimers at steps through adsorbate-adsorbate steric repulsion or back bond weakening.[12,28] This gives rise to rougher steps.

IV. CONCLUSIONS

Analysis of the equilibrium shapes of Si islands and pits demonstrates that their aspect ratio depends on their size. This is because the intrinsic surface-stress anisotropy drives features to have a greater aspect ratio as they grow. We were able to calculate the ratio of step free energies, F_b/F_a, and the ratio of average step free energy to strain energy, $\sqrt{F_aF_b}/E_s$. Experiment shows that the addition of 0.1 ML Cl to Si(100)-(2×1) destabilizes the step edges, resulting in rougher S_B steps than seen for clean Si(100). Hence, there is

a higher ratio of step free energies when Cl is present and the surface is in equilibrium. The observed higher ratio of step free energies for pits compared to islands is attributed to the higher Cl concentration on the terraces than on the RI's. The adsorbates have a similar effect on the step free energy and surface-stress so that the ratio of average step free energy to the strain energy is unaltered after the surface is modified by Cl adsorbates.

This study, emphasizing an ''ungrowth'' process, complements previous work on step energies that focused on a ''growth'' process. For the first time, we were able to deal quantitatively with step free energies in a true equilibrium state after surface roughening. This is a significant transition from a qualitative to a quantitative description of the effects of halogens on Si surfaces.

ACKNOWLEDGMENTS

This paper was supported by the National Science Foundation and the U.S. Department of Energy, Division of Materials Sciences under Award No. DEFG02-91ER45439, through the Frederick Seitz Materials Research Laboratory at the University of Illinois at Urbana-Champaign. The experiments were performed in the Center for Microanalysis of Materials, and we gratefully acknowledge the expert assistance of V. Petrova, S. Burdin, and E. Sammann. S.V.K. thanks Professor F. Liu for comments about Ref. 14.

*Permanent address: Institute of Materials Science and Technology (INTEMA), Universidad Nacional de Mar del Plata-CONICET, Juan B. Justo 4302, B7608FDQ Mar del Plata, Argentina.

[1] H.J.W. Zandvliet, Rev. Mod. Phys. **72**, 593 (2000).

[2] B.S. Swartzentruber, Y.-W. Mo, R. Kariotis, M.G. Lagally, and M.B. Webb, Phys. Rev. Lett. **65**, 1913 (1990).

[3] N.C. Bartelt, R.M. Tromp, and E.D. Williams, Phys. Rev. Lett. **73**, 1656 (1994).

[4] H.J.W. Zandvliet, H.B. Elswijk, E.J. van Loenen, and D. Dijkkamp, Phys. Rev. B **45**, 5965 (1992).

[5] V. Zielasek, F. Liu, Y. Zhao, J.B. Maxson, and M.G. Lagally, Phys. Rev. B **64**, R201320 (2001) used low-energy electron microscopy to study morphology changes of an island during homoepitaxial growth on Si(100). They used a Si_2H_6 gas source to grow at less than 1 ML in 10 min.

[6] C.M. Aldao and J.H. Weaver, Prog. Surf. Sci. **68**, 189 (2001).

[7] K.S. Nakayama, E. Graugnard, and J.H. Weaver, Phys. Rev. Lett. **88**, 125508 (2002).

[8] C.F. Herrmann, D. Chen, and J.J. Boland, Phys. Rev. Lett. **89**, 096102 (2002).

[9] G.J. Xu, E. Graugnard, V. Petrova, K.S. Nakayama, and J.H. Weaver, Phys. Rev. B **67**, 125320 (2003).

[10] G.J. Xu, K.S. Nakayama, B.R. Trenhaile, C.M. Aldao, and J.H. Weaver, Phys. Rev. B **67**, 125321 (2003).

[11] G.J. Xu, E. Graugnard, B.R. Trenhaile, K.S. Nakayama, and J.H. Weaver, Phys. Rev. B **68**, 075301 (2003).

[12] C.M. Aldao, S.E. Guidoni, G. J. Xu, K.S. Nakayama, and J.H. Weaver (unpublished).

[13] M. Fehrenbacher, H. Rauscher, and R.J. Behm, Surf. Sci. **491**, 275 (2001).

[14] A. Li, F. Liu, and M.G. Lagally, Phys. Rev. Lett. **85**, 1922 (2000).

[15] Y.-W. Mo, B.S. Swartzentruber, R. Kariotis, M.B. Webb, and M.G. Lagally, Phys. Rev. Lett. **63**, 2393 (1989).

[16] W. Świech and E. Bauer, Surf. Sci. **255**, 218 (1991).

[17] D.C. Schlösser, L.K. Verheij, G. Rosenfeld, and G. Comsa, Phys. Rev. Lett. **82**, 3843 (1999).

[18] S. Kodambaka, V. Petrova, S.V. Khare, D.D. Johnson, I. Petrov, and J.E. Greene, Phys. Rev. Lett. **88**, 146101 (2002); S. Kodambaka, S.V. Khare, V. Petrova, D.D. Johnson, I. Petrov, and J.E. Greene, Phys. Rev. B **67**, 035409 (2003).

[19] K. Nakayama, C.M. Aldao, and J.H. Weaver, Phys. Rev. B **59**, 15 893 (1999).

[20] J.G. McLean, B. Krishnamachari, D.R. Peale, E. Chason, J.P. Sethna, and B.H. Cooper, Phys. Rev. B **55**, 1811 (1997).

[21] N.C. Bartelt and R.M. Tromp, Phys. Rev. B **54**, 11 731 (1996).

[22] S.V. Khare, S. Kodambaka, D.D. Johnson, I. Petrov, and J.E. Greene, Surf. Sci. **522**, 75 (2003).

[23] O.L. Alerhand, A.N. Berker, J.D. Joannopoulos, D. Vanderbilt, R.J. Hamers, and J.E. Demuth, Phys. Rev. Lett. **64**, 2406 (1990).

[24] M.T. Middel, H.J.W. Zandvliet, and B. Poelsema, Phys. Rev. Lett. **88**, 196105 (2002) used STM to study pits on Ge(100) at room temperature after ion bombardment at $\sim$300 K and annealing for 1 min at 400–700 K.

[25] V.L. Spiering, S. Bouwstra, and R. Spiering, Sens. Actuators A **39**, 149 (1993).

[26] H.J.W. Zandvliet and H.B. Elswijk, Phys. Rev. B **48**, 14 269 (1993).

[27] H.J.W. Zandvliet, S. van Dijken, and B. Poelsema, Phys. Rev. B **53**, 15 429 (1996).

[28] V.P. Zhdanov and B. Kasemo, Phys. Rev. B **56**, R10 067 (1997).